PLOS Complex Systems

RESEARCH ARTICLE

Multiscale mobility: How the COVID-19 pandemic reshaped Mexico's intermunicipal connectivity

Issa Moussa Diop[1], Erika Cruz-Bonilla[2], Christian Wolff[3], Hocine Cherifi[4], Maribel Hernández-Rosales[2]*

1 DS4H, I3S, Université Côte d'Azur, Nice, France, **2** Center for Research and Advanced Studies of Polytechnic National Institute, Irapuato Unit, Libramiento Norte Carretera Irapuato León Kilómetro 6, Irapuato, Guanajuato, Mexico, **3** Mainz University of Applied Sciences, Mainz, Germany, **4** ICB, UMRCNRS, Université de Bourgogne, Dijon, France

* maribel.hr@cinvestav.mx

OPEN ACCESS

Citation: Diop IM, Cruz-Bonilla E, Wolff C, Cherifi H, Hernandez-Rosales M (2026) Multiscale mobility: How the COVID-19 pandemic reshaped Mexico's intermunicipal connectivity. PLOS Complex Syst 3(1): e0000086. https://doi.org/10.1371/journal.pcsy.0000086

Editor: Ruiqi Li, Beihang University, CHINA

Received: March 11, 2025

Accepted: December 20, 2025

Published: January 20, 2026

Data availability statement: The mobility network data is available in https://osf.io/42xqz/files/osfstorage.

Funding: This work was supported by the Fondo Conjunto de Cooperación México-Uruguay de la Agencia Uruguaya

Abstract

Mobility networks are vital for economic activity, social interaction, and urban development, yet they remain highly vulnerable to external shocks. The COVID-19 pandemic profoundly disrupted human mobility, but most studies have focused on short-term responses or macroscopic patterns, leaving long-term structural transformations underexplored. Here, we analyze Mexico's intermunicipal mobility network from 2020 to 2021 using a mesoscopic decomposition framework that distinguishes local (short-distance) components from global (long-distance) connections. This multiscale approach moves beyond static or node-level metrics to reveal how connectivity itself was reshaped. Clustering analysis and change point detection further uncover temporal shifts in mobility dynamics. Our results show three clear phases. Before the pandemic, the network was dense and highly connected. During the pandemic, mobility fragmented into smaller, locally cohesive clusters, reflecting sharp declines in long-distance travel. After restrictions eased, mobility partially recovered but never fully returned to its pre-pandemic structure, indicating lasting behavioral and structural shifts. Regional disparities were pronounced: western and northwestern regions showed greater resilience, while southeastern regions remained fragmented longer. Broader lifestyle changes—including remote work, digitalization, and e-commerce—reinforced local clustering and weakened interregional ties, pointing to a durable reconfiguration of mobility networks. By integrating a temporal, multiscale perspective, this study reveals how crises reshape both local cohesion and interregional connectivity. Beyond documenting disruption, it shows that mobility systems do not simply "bounce back." Instead, they reorganize, often unevenly, underscoring the urgency for adaptive transport policies, resilient urban planning, and digital infrastructure capable of supporting mobility in a permanently altered landscape. These insights provide a data-driven foundation for future mobility resilience strategies.

de Cooperación Internacional (AUCI) and the Agencia Mexicana de Cooperación Internacional para el Desarrollo (AMEXCID) (Mexico–Uruguay Joint Cooperation Fund, through the Uruguayan Agency for International Cooperation (AUCI) and the Mexican Agency for International Development Cooperation (AMEXCID)) (to MHR). The funders had no role in study design, data collection and analysis, decision to publish, or preparation of the manuscript.

Competing interests: The authors have declared that no competing interests exist.

Author summary

Human mobility shapes economic activity, transportation systems, and social interactions. The COVID-19 pandemic disrupted mobility patterns worldwide, modifying movement within and between regions. This study analyzes the impact of the pandemic on Mexico's intermunicipal mobility network by examining connectivity changes at local, regional, and national scales. Mobility data from 2020 and 2021 capture key phases of disruption, adaptation, and partial recovery. The results highlight the long-term structural impacts of the crisis on mobility dynamics. Our research shows that while some travel habits have bounced back to pre-pandemic levels, others have shifted for good. Short trips between neighboring towns are on the rise, but long-distance travel is taking longer to recover, signaling a reshaping of regional mobility. In some areas, the disruption is more persistent, shaped by differences in infrastructure, local economies, and everyday travel choices. Rather than snapping back to "normal," mobility networks are gradually evolving, as revealed by our clustering analysis. The pandemic has left a lasting imprint on how people move. These findings matter for the future of cities and transportation. They highlight the urgent need for flexible, resilient systems that can withstand future shocks. They also point to the growing power of digital infrastructure—remote work and online shopping are changing daily movement in ways that reduce travel demand. By understanding how mobility networks react to crises, policymakers can craft strategies that not only keep people connected but also push toward long-term sustainability. Our framework offers a valuable tool for studying these shifts and building smarter, more resilient transportation systems.

Introduction

The study of mobility networks provides a powerful framework for understanding societal dynamics [1]. These networks integrate transportation, communication, and migration systems, capturing not only the physical movement of people and goods but also the social, economic, and cultural interactions that shape human behavior. Investigating how mobility patterns emerge, evolve, and influence network structures is essential for improving efficiency, strengthening resilience, and mitigating systemic vulnerabilities. A diverse range of data sources supports this research, including mobile phone location data, GPS tracking, social media, mobile applications, OpenStreetMap, and city-specific portals [2–5]. The COVID-19 pandemic underscored the importance of these approaches. As a global crisis that disrupted nearly every aspect of daily life, it generated an unprecedented surge of scientific research across disciplines, with human mobility analysis emerging as a central focus due to its direct implications for epidemiology and public health. Studies consistently demonstrated how mobility shifts influenced infection dynamics and broader societal processes [6–11]. This body of work highlighted not only the short-term consequences of restrictions but also the long-term reorganization of movement patterns, providing critical insights into resilience, adaptation, and structural change. At larger and intermediate scales, prior research established the structural properties of mobility networks

and how they were disrupted during the pandemic. Early analyses revealed spatial community patterns, modularity, and stability in human mobility [12–14], while subsequent studies documented sharp declines in travel following non-pharmaceutical interventions in contexts such as the U.S. and Tokyo [15,16]. Systematic reviews confirmed the ubiquity of these trends, emphasizing both the importance of individual-level data and the need for analyses extending beyond the peak of the pandemic [17], aligning with broader findings that interventions reshaped mobility everywhere, though recovery trajectories varied by context [15,16,18,19]. Spatial and socioeconomic heterogeneity were also consistent themes. Reductions in mobility were generally more severe in dense urban areas than in rural regions, with recovery strongly conditioned by trip purpose [20]. Longer-term lifestyle shifts further reshaped mobility patterns: suburbanization, digitalization, and altered commuting behaviors persisted long after restrictions were lifted, with uneven effects across cities and countries [21]. Reviews confirmed that while some indicators, such as trip frequency and radius of gyration, returned to pre-pandemic values, others—notably home-dwell time and public transport use—settled into new equilibria, signaling a "new normal" [18,19]. These changes were accompanied by increases in car ownership and cycling, declines in sharing services, and widespread adoption of hybrid work models. Socioeconomic variation further shaped these dynamics: in the UK, rural low-income regions exhibited larger spatial shifts in travel, whereas urban high-income groups experienced primarily temporal adjustments [22]. In Mexico, Fontanelli et al. [23] showed that intermunicipal networks during 2020–2021 reflected both the direct effects of the pandemic and population size. Building on this literature, we examine Mexico's intermunicipal mobility network using mesoscopic component analysis [24]. This method partitions the network into dense local components that represent short-distance movements and global components that link them through long-distance travel. By applying this approach across pre-pandemic, pandemic, and post-restriction periods, we assess how external shocks such as health restrictions and urbanization reshaped both local clustering and interregional connectivity. Our results show that mobility partially recovered but did not fully return to its pre-pandemic structure, underscoring the long-term behavioral and structural changes that large-scale crises imprint on human mobility.

Results

Mobility network transformations: Structural shifts, clustering, and long-term impacts

Mobility networks evolve dynamically in response to external shocks, yet large-scale crises can trigger enduring structural transformations. Fig 1 illustrates the temporal evolution of key network properties, highlighting how the COVID-19 pandemic reshaped intermunicipal connectivity. Red dashed lines denote statistically significant change points, marking shifts in mobility dynamics. These changes were not uniform: different metrics capture distinct aspects of the network, revealing heterogeneous impacts on density, clustering, and long-range connectivity.

The first change appears in February–March 2020, shortly before the first confirmed case (Feb 27) and WHO's pandemic declaration (March 11). Network density and shortest path length drop sharply, indicating early adaptation and reduced connectivity. The second change occurs in June–July 2020, during the post-lockdown transition. Transitivity and assortativity decline, while clustering and density remain low. This suggests network fragmentation and weaker global cohesion. A third shift is visible in September–October 2020, during Mexico's second wave and a PAHO alert (October 9). Shortest path increases, clustering and transitivity fluctuate, and assortativity drops. The network restructures in response to renewed restrictions. The fourth change emerges between April and June 2021, following the vaccination campaign for educators. Clustering rises, reflecting stronger local structures. Assortativity declines, suggesting a breakdown in degree-based connections. A fifth transition occurs on September 16, 2021 (Independence Day). Transitivity, clustering, and density fluctuate, likely due to mass travel for public celebrations. In total, five transitions align with key policy actions or epidemiological escalations (Table 1). This confirms the link between public health policies and mobility network evolution.

To explore these transitions further, we apply clustering to daily topological metrics. Fig 2 presents the results.

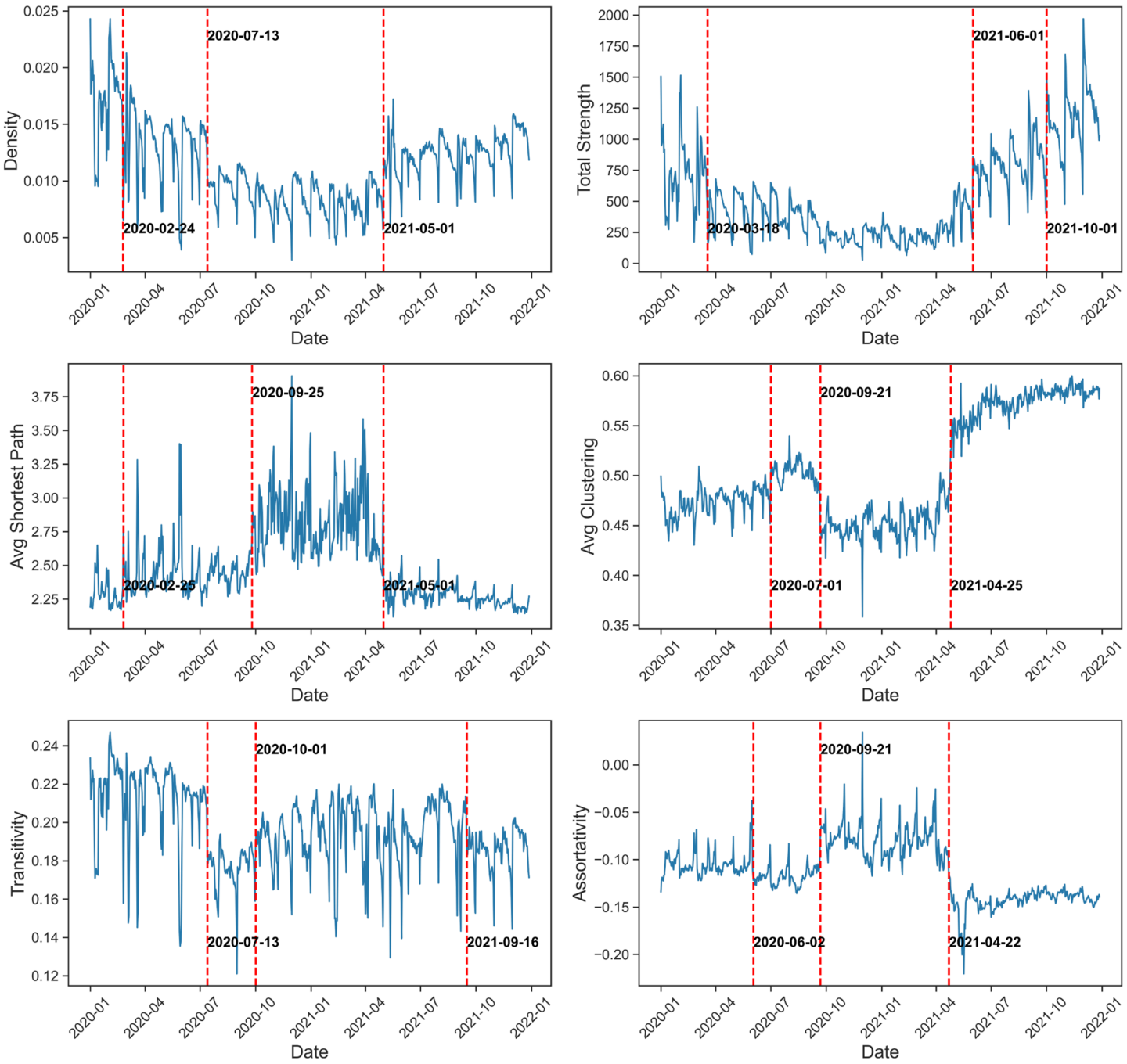

Fig 1. **Temporal evolution of intermunicipality Mexico network metrics with detected change points.** This figure presents the temporal evolution of various metrics over time. Each subplot corresponds to a different metric, with the x-axis representing time (dates) and the y-axis indicating the respective metric values. The red dashed vertical lines highlight significant change points, annotated with their corresponding dates.

https://doi.org/10.1371/journal.pcsy.0000086.g001

The silhouette score indicates that $k = 2$ or $k = 3$ are suitable choices for the number of clusters. We select $k = 3$ because of the clear and strong separation observed among the three clusters. Fig 2 A displays the PCA projection of daily networks, where each point corresponds to a day, colored by month. Three distinct clusters emerge, revealing a

Table 1. Key COVID-19 policy milestones in Mexico from 2020 to 2021. Events are compiled from official government sources and public health reports [25–28].

Date	Event/Measure
Dec, 2019	China reported an outbreak of pneumonia of unknown cause in Wuhan, with 27 cases.
Jan 9, 2020	Identification of a novel coronavirus announced.
Jan 11–12, 2020	First death caused by the disease reported.
Jan 30, 2020	WHO declares a Public Health Emergency of International Concern (PHEIC).
Feb 27, 2020	First confirmed COVID-19 case detected in Mexico.
Feb 28, 2020	First COVID-19 case officially registered in Mexico's health platform.
Mar 11, 2020	WHO declares COVID-19 a global pandemic.
Mar 18, 2020	First COVID-19 death registered in Mexico.
Mar 23, 2020	Launch of the National Healthy Distance Campaign and implementation of sanitary and social distancing measures.
Apr 1, 2020	National emergency declared; Mexico enters Phase 3 of the pandemic.
May 13, 2020	"Return to the New Normality" plan announced.
Jun 1, 2020	Resumption of essential economic activities begins.
Oct 9, 2020	PAHO/WHO issues epidemiological alert regarding new wave of COVID-19 outbreaks.
Nov 2, 2020	Day of the Dead celebrations in Mexico lead to a rise in cases.
Dec 12, 2020	Basilica of Guadalupe closed; authorities urged virtual celebration to prevent pilgrimages and contagion.
Dec 24, 2020	Christmas celebrated amid rising infections and hospitalizations in Mexico and globally.
Dec 24, 2020	Mexico begins its National Vaccination Campaign with the first Pfizer-BioNTech doses, prioritizing frontline medical staff.
Dec 31, 2020	Government advises people to celebrate New Year's Eve only with household members.
Jan 21, 2021	Mexico records its highest single-day number of new cases: 22,339.
Feb 14, 2021	Nationwide COVID-19 vaccination campaign begins for the elderly population.
Mar 15, 2021	More states shift from "Red" (maximum alert) to "Orange" under the traffic light system.
Apr 12, 2021	Vaccination campaign expands to educational personnel in preparation for school reopening.
May 17, 2021	Mexico City moves to "Yellow" status; restrictions ease, including public gatherings and some commercial activity.
Jun 7, 2021	First week since the start of the pandemic where no state is under "Red" status.
Jul 26, 2021	Delta variant prompts new restrictions in some regions; Mexico City reverts to "Orange".
Aug 30, 2021	Return to in-person classes nationwide under strict protocols.
Sep 16, 2021	National celebrations for Independence Day proceed with partial in-person events and increased mobility.
Oct 18, 2021	Mexico City returns to "Green" status for the first time since early 2020.
Nov 3, 2021	COVID-19 vaccination starts for adolescents aged 12–17 with comorbidities.
Dec 6, 2021	Booster shots begin for individuals aged 60 and older.

https://doi.org/10.1371/journal.pcsy.0000086.t001

more nuanced segmentation of pandemic dynamics. Cluster 1 dominates the pre-pandemic and early disruption phase (January–June 2020). Cluster 2 takes over during the prolonged restriction period (July 2020 to March 2021). It aligns with the implementation of the Epidemiological Traffic Light System and the first vaccination campaigns. Cluster 3 emerges from April 2021 onward, characterizing the recovery phase with more stabilized structural configurations.

The temporal heatmap in Fig 2B confirms these patterns. Cluster 1 disappears entirely from July 2020 to March 2021 and reappears only marginally afterward. Cluster 2 dominates during the disruption phase, especially in early 2021, while Cluster 3 becomes predominant from mid-2021. This segmentation shows that structural mobility regimes align closely with policy shifts and recovery stages, rather than raw mobility volume.

Building on this discussion of long-term mobility shifts, a comparative analysis of network properties provides further insights into the evolution of intermunicipal connectivity during 2020 and 2021. Fig 3 compares key network metrics, uncovering trends and structural changes driven by mobility restrictions and their gradual relaxation. This visualization emphasizes how multiple metrics evolve jointly across months and years, offering a dynamic perspective on how structural properties co-vary under different temporal regimes.

Examining the relationship between total strength and average clustering coefficient provides further insight into the structural evolution of mobility patterns. A month-by-month analysis of strength and density reveals a sharp drop in connectivity starting in April 2020, coinciding with the National Healthy Distance Campaign (March 23) and the national emergency declaration (April 1), as noted in Table 1. This collapse in total strength and density reflects the immediate effect

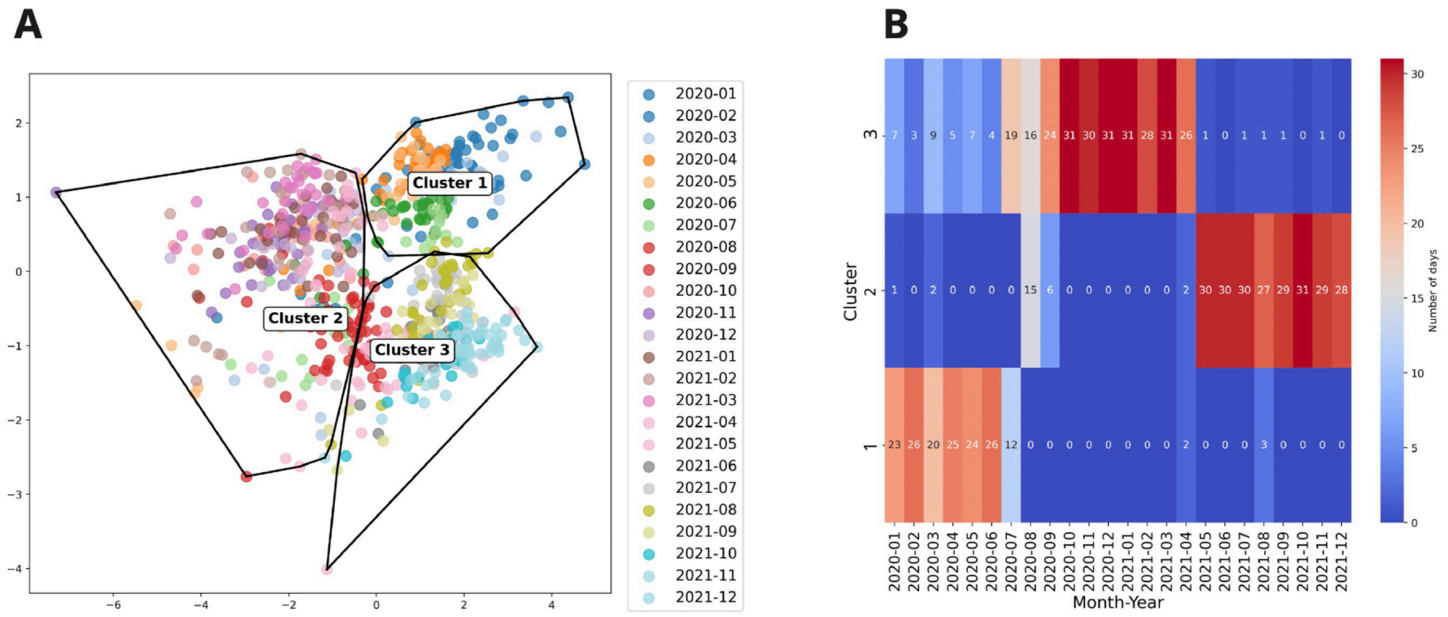

Fig 2. Temporal evolution of the Mexico intermunicipal mobility network structures. (A) Clustering results of daily mobility network structures projected into a reduced-dimensional space. Each point represents a day, colored according to its corresponding month. The black convex hulls indicate the boundaries of the detected clusters. (B) Heatmap showing the temporal distribution of clusters. The x-axis represents months, while the y-axis corresponds to clusters. The color intensity indicates the number of days assigned to each cluster within a given month.

https://doi.org/10.1371/journal.pcsy.0000086.g002

of strict lockdown measures and voluntary behavioral adaptation. Following this initial shock, we observe a gradual and irregular recovery. Notably, strength and density remain significantly below pre-pandemic levels throughout the second half of 2020—even during periods such as August–October, when movement restrictions were partially relaxed. A significant and sustained increase is observed from April 2021 onward, coinciding with the expansion of the national vaccination campaign (March–May 2021), school reopening preparations (April), and the easing of restrictions in major regions like Mexico City (May 17). During the second half of 2021 (July–December), strength and density stabilize at their highest values since the onset of the pandemic. However, density remains below pre-pandemic levels, highlighting that even though mobility intensity has returned, the structure of connectivity has changed. These findings reinforce the idea that long-term behavioral changes, such as remote work, regionalization of activity, and reduced long-distance commuting, have permanently altered network organization. The pairwise scatter plots in Fig 3 further clarify this transition. In 2020, the relationship between total strength and average clustering coefficient shows a dispersed pattern, especially between April and October, where clustering fluctuates despite lower strength levels. By contrast, in 2021, a much tighter relationship emerges, especially from July to December, where the clustering coefficient stabilizes at high levels (around 0.58 and 0.6) regardless of total strength. This indicates a restructuring of local connectivity: even when overall mobility is not at its maximum, trips are increasingly concentrated within tightly knit local communities, which could reflect a preference for proximity-based movement or the consolidation of urban and peri-urban networks. Finally, the contrast between early 2020 (January–March) and late 2021 (November–December) is striking. While total strength in both periods may appear comparable, their network signatures differ: late 2021 exhibits higher clustering and moderate density, pointing to a qualitatively different spatial organization of mobility. These results underscore that the pandemic not only affected how much people moved, but also how they were connected through space.

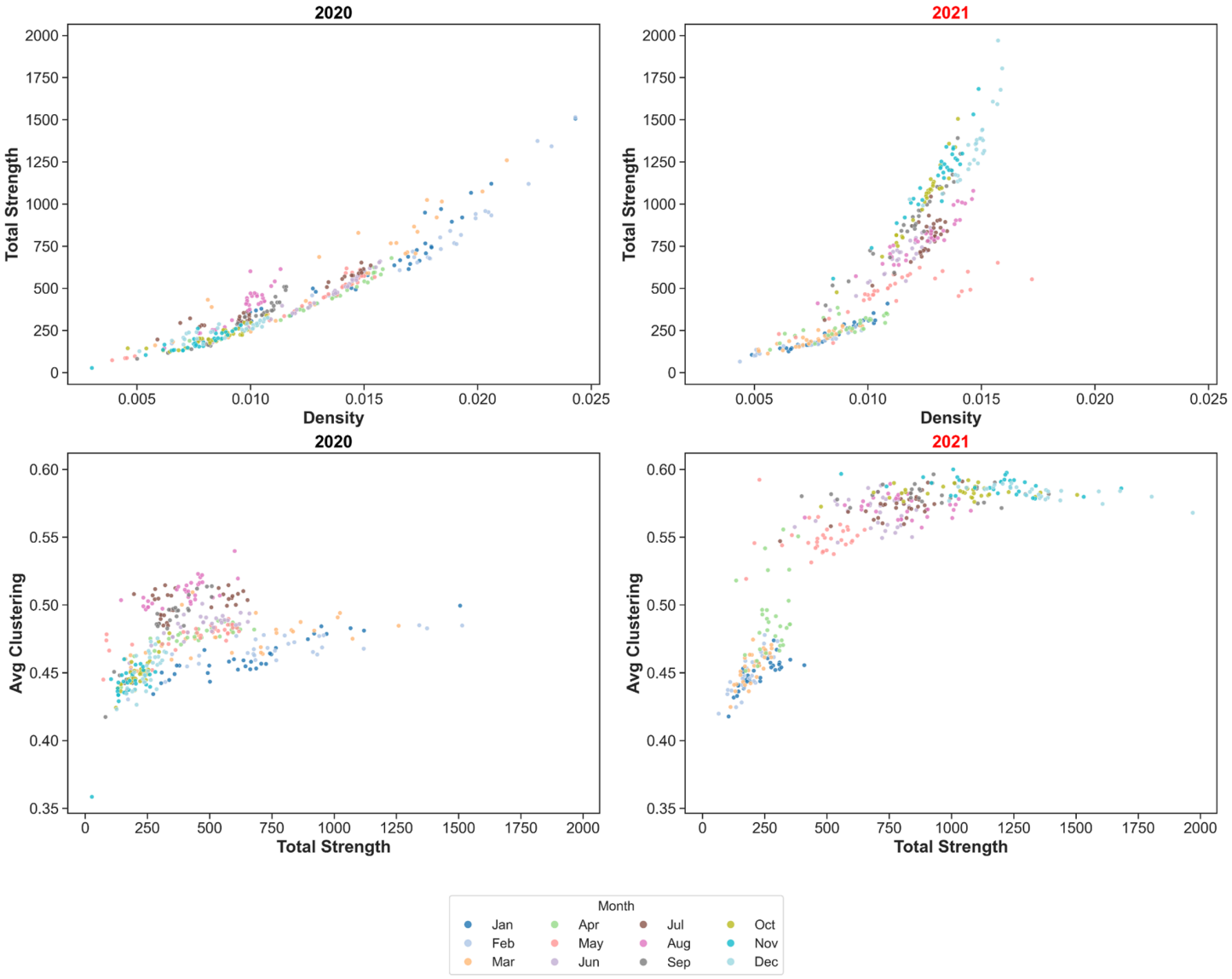

Fig 3. Monthly joint evolution of structural metrics in Mexico's intermunicipal mobility network (2020–2021). The scatter plots display relationships between Density, Total Strength, and between Total Strength and Average Clustering Coefficient, with data points colored according to the month. Each subplot shows the relationship between two structural metrics, separately for 2020 (left column) and 2021 (right column). Each dot represents one day, and its color encodes the corresponding month. The monthly color encoding allows us to observe seasonal dynamics, shifts in structural regimes, and changes in variability or dispersion between pandemic phases.

https://doi.org/10.1371/journal.pcsy.0000086.g003

Dynamics of local components: Stability, fragmentation, and regional mobility patterns

The detection of local components in Mexico's intermunicipal mobility network ranges from 7 to 40, with an average of 13. The size of these components, defined by the number of municipalities within each, varies considerably, as illustrated in Fig 4A.

The highest number of components occurs on November 30, 2020, while the lowest is recorded on May 26, 2020. Indeed, November 30, 2020, represents an exceptional case. Just days earlier, Mexico experienced a peak in COVID-19 cases, likely prompting a reduction in travel (Fig 4). On the same date, a solar eclipse occurred [29], which in some

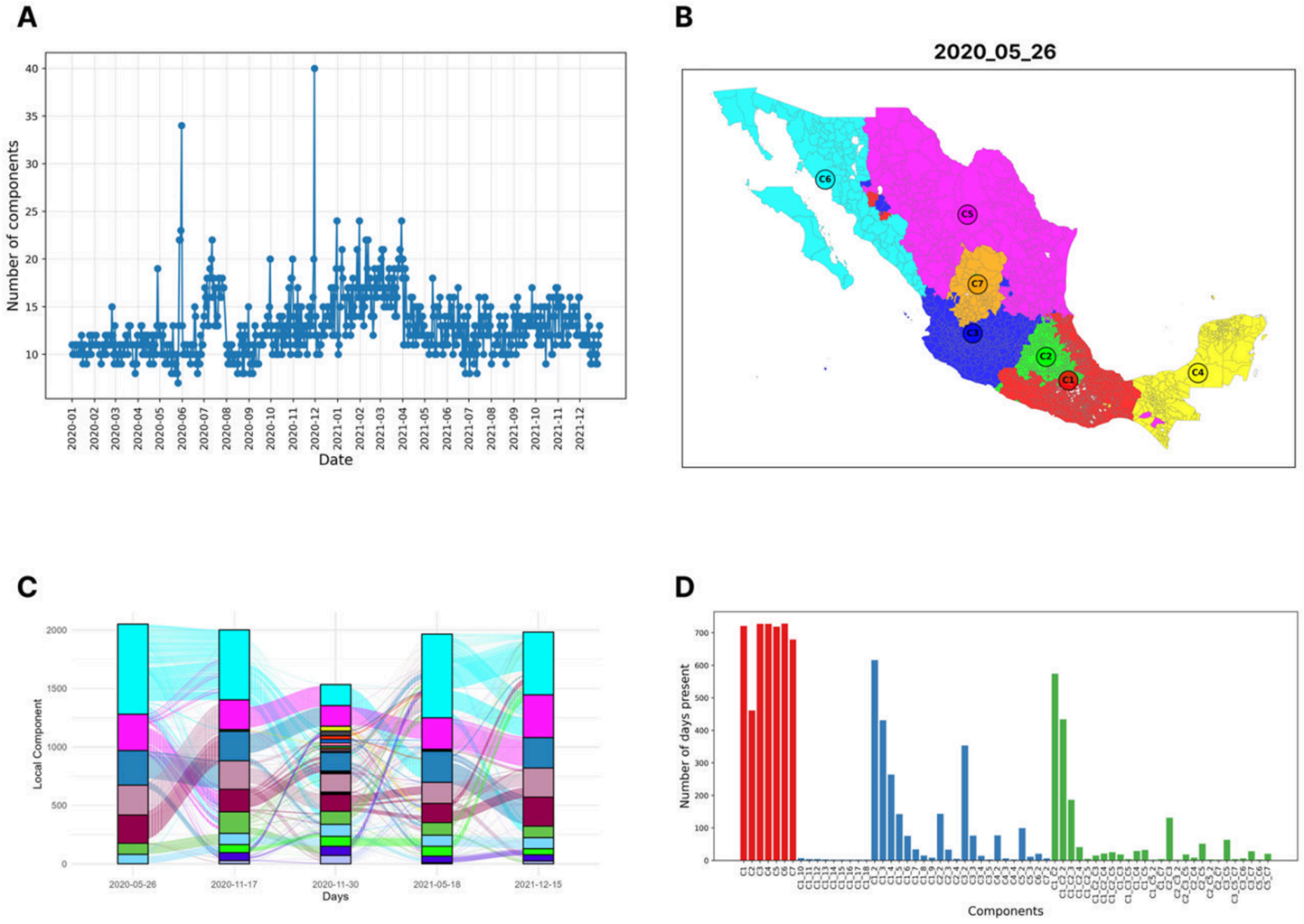

Fig 4. Temporal and structural evolution of local components in Mexico's intermunicipal mobility network. (A) Number of network components over time, highlighting fluctuations in connectivity throughout the pandemic. Peaks correspond to periods of increased fragmentation, likely due to mobility restrictions. (B) Spatial distribution of major local components on May 26, 2020, revealing the geographic segmentation of mobility networks. The base map was created with GeoPandas using INEGI's publicly available shapefiles [30]. (C) Sankey-like diagram showing the temporal evolution of predefined groups of municipalities corresponding to local components identified on the reference day (the day with the fewest components). The flows illustrate how these municipalities are reassigned across daily-detected components on five key dates, capturing the persistence, fragmentation, or merging of mobility structures over time. (D) Distribution of component persistence, indicating how long each local component remained stable. Red bars represent the most persistent components, blue bars represent fragmented components, and green bars show merged components.

https://doi.org/10.1371/journal.pcsy.0000086.g004

regions may have discouraged mobility due to cultural beliefs. Additionally, Interjet, a major national airline responsible for numerous domestic routes, suspended operations on that day, limiting travel options. The convergence of these factors contributed to an unusual fragmentation of the mobility network, reflected in the elevated number of components.

As shown in Fig 4B, the seven major local components align with Mexico's economic and cultural regions [31]: East, Southwest, Center-South, West, Southeast, Northeast, Northwest, and Center-North. In our analysis, the East and Southwest regions often cluster together.

Most components are small, with 52% containing fewer than 100 municipalities. The second most common size range is 200–300 municipalities (23%), while the largest components include between 600 and 700 municipalities. This variation

is significant, considering that Mexican states have an average of 77 municipalities. However, some states such as Oaxaca (570), Puebla (217), Veracruz (212), Jalisco (125), and the State of Mexico (125) [32], have a much higher number, contributing to the formation of large components.

Despite these variations, local component sizes remain relatively stable over time, with most staying within the small to mid-size range. However, there are deviations, including a decline in June 2020 and peaks between December 2020–February 2021 and May–July 2021. These fluctuations reflect the impact of quarantine measures, holiday travel, and the relaxation of movement restrictions. The municipal composition of these components also remains relatively stable, with changes primarily influenced by network size and the formation of sub-communities. For example, Oaxaca appears consistently as an independent component. However, on November 17, 2020, smaller sub-components emerge within it and in central Mexico. On low-mobility days, the network becomes more fragmented, increasing the number of small components, as observed in Fig 4C. This figure tracks the municipalities initially belonging to each component and follows their daily reassignments over five key dates. These changes reflect the structural instability or cohesion of mobility patterns. Conversely, on high-mobility days, sub-communities within larger components become more visible, particularly in metropolitan areas.

Fig 4D confirms that among the seven main components (C1 to C7), C3, C4, and C6 remain the most stable. These components retain at least 80% of their original size over time. The spatial distribution of major local components on May 26, 2020, serves as the baseline for geographic segmentation (Fig 4B). In contrast, C1 and C2 exhibit the highest fragmentation tendency. These components are frequently split into multiple sub-components or merge with others. The most unstable components concentrate in the East-Southwest and Southeast regions. These regions contain a significantly higher number of municipalities than the national average. Prior research indicates that certain regions tend to form functional mobility clusters in response to emergent situations, such as pandemics or economic disruptions. This is very often the case in Oaxaca, the state with the largest number of municipalities (570) in the Southwest region of Mexico.

Fig 5 illustrates change points in Component 3. Similar patterns are observed in Components 4 and 6 (see S2 Fig and S3 Fig). All three exhibit a major change in March–April 2020. This coincides with national restrictions such as the Healthy Distance Campaign (March 23) and the emergency declaration (April 1). Metrics like density and strength drop, reflecting rapid connectivity loss. A second shift occurs in late June to early July 2020. This corresponds to the reopening phase. In Component 3, clustering and transitivity change markedly. Component 4 shows more stability, indicating region-specific responses. A third transition takes place between January and April 2021. This period aligns with vaccine rollouts. Clustering increases while assortativity decreases. These changes reflect adaptation rather than a full return to pre-pandemic configurations. Component 6 continues its structural reorganization through August. A final transition appears between June and August 2021, before Mexico's Independence Day (September 16). Components 4 and 6 shift earlier than the national network. This indicates possible regional anticipation of policy changes. Overall, breakpoints align with national trends, but their effects vary. Average clustering, transitivity, and assortativity evolve differently across regions. This underscores the need for disaggregated mobility analyses.

Further analysis using clustering techniques (Fig 6) reveals regional disparities in mobility responses throughout the pandemic. Unlike the national network, which exhibited a marked divergence between pre- and post-restriction phases, regional mobility patterns appear more resilient and quicker to stabilize.

In the Western region (Component 3), clustering analysis reveals two structural regimes. Cluster 1 dominates the early phase of the pandemic (January–May 2020) and reappears as the main regime from mid-2021 onward. In contrast, Cluster 2 prevails from June 2020 to April 2021, reflecting the period of strongest disruptions. The transition visible in the heatmap (Fig 6A, right panel) shows a sharp switch around June 2021, after which most months are reassigned to Cluster 1. This suggests a recovery of pre-pandemic mobility structure in this region, particularly regarding clustering and density levels. This interpretation is supported by the stabilization of the clustering coefficient and assortativity in the second half of 2021.

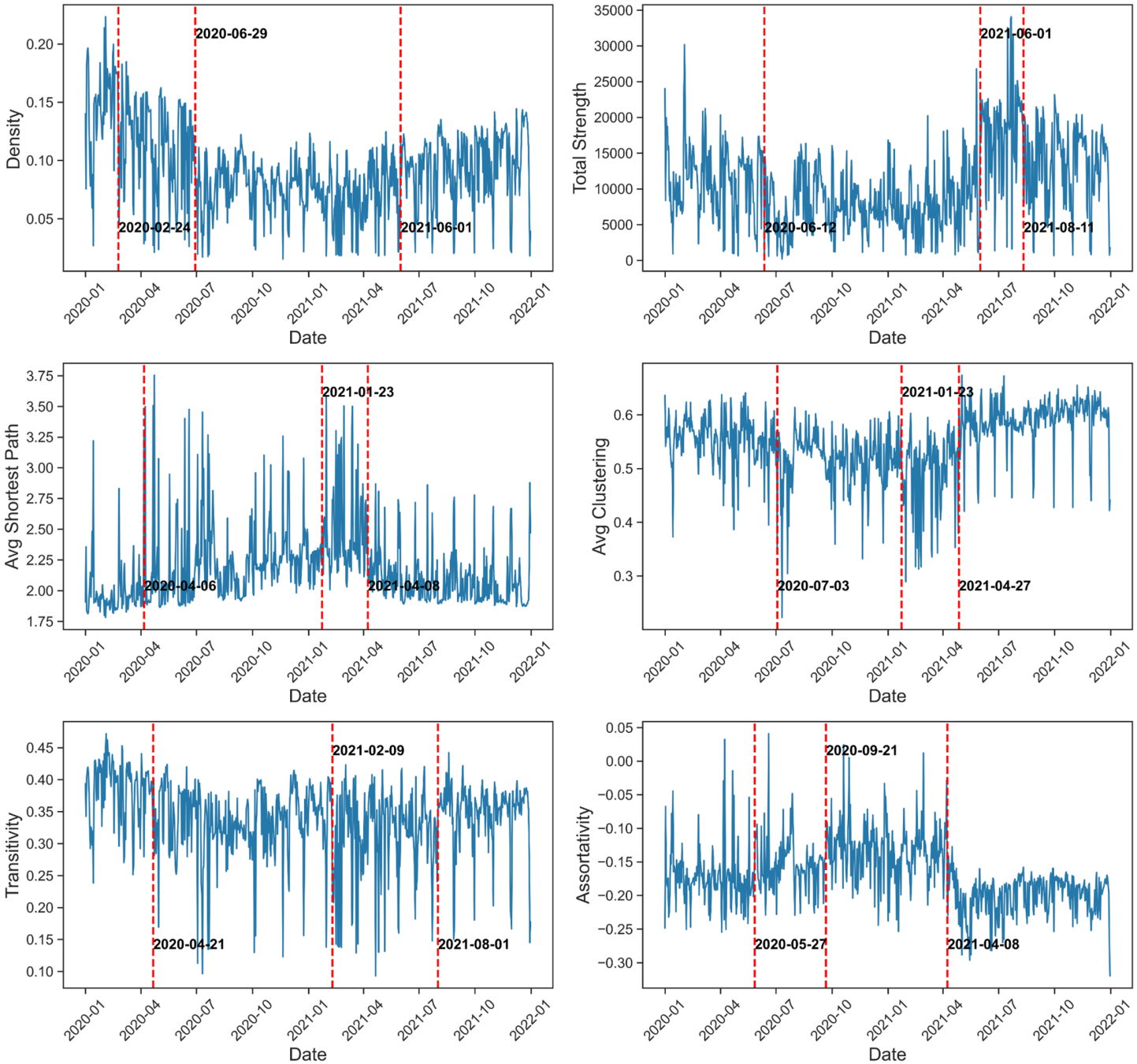

Fig 5. **Temporal evolution of the local component in the Western Region with detected change points.** Each subplot represents a different metric, with the x-axis indicating time (dates) and the y-axis showing respective metric values. Red dashed vertical lines highlight significant change points annotated with their corresponding dates.

https://doi.org/10.1371/journal.pcsy.0000086.g005

In the Northwest region (Component 4), the dynamics differ slightly. Cluster 1 is dominant both before the pandemic and in the late phase (mid to late 2021), while Cluster 2 dominates the intermediate disruption period from April 2020 to April 2021. However, the temporal boundary between clusters is less sharp than in the West. Notably, some months

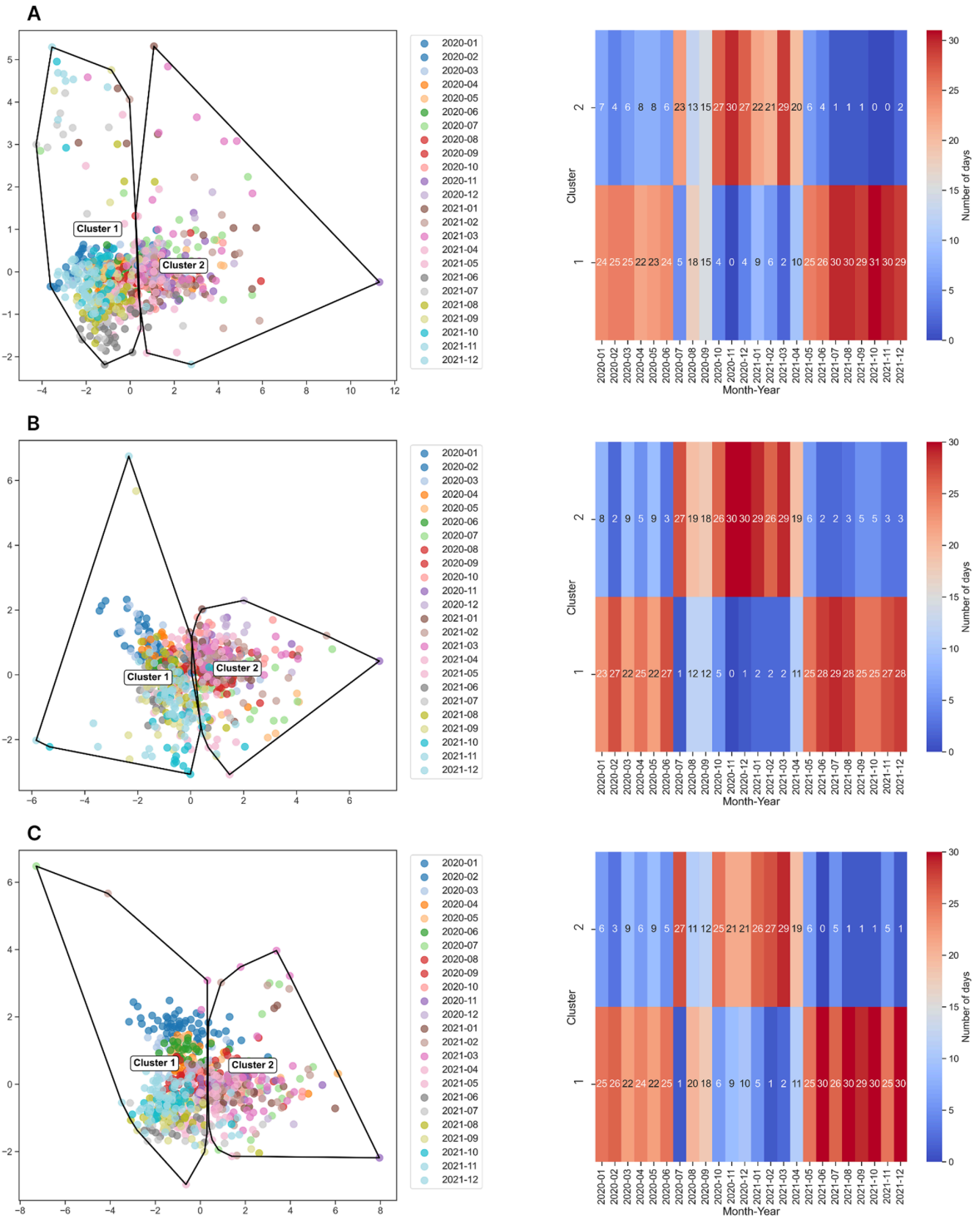

Fig 6. **Clustering of the stable local components.** (Left) Clustering results of daily mobility network structures projected into a reduced-dimensional space. Each point represents a day, colored by month. The black convex hulls indicate the boundaries of detected clusters. (Right) Heatmap showing the temporal distribution of clusters, with the x-axis representing months and the y-axis corresponding to clusters. Color intensity indicates the number of days assigned to each cluster within a given month. (A) represents the West region, (B) represents the South-East region, and (C) represents the North-West region.

https://doi.org/10.1371/journal.pcsy.0000086.g006

in late 2021 show mixed membership. This suggests that, although mobility intensity recovers (as seen in strength and density), topological structures remain altered, particularly with lower clustering and persistently negative assortativity.

In the Southeast region (Component 6), the transition is more gradual. Cluster 1 represents the initial pandemic period and early 2021, while Cluster 2 becomes the dominant regime from May 2021 onward. The prolonged presence of Cluster 2 suggests a structural reorganization of the mobility network in this region. The increased cohesion observed in this phase, evident in the rise of clustering and transitivity, reflects more localized and resilient mobility patterns that differ from both pre-pandemic and disruption-phase behaviors (see Figs 7 and S1 Fig).

Overall, the regional clustering results reveal that while all three components experienced disruptions, their recovery trajectories differ. The Western region exhibits a near-complete return to pre-pandemic structure. The Northwest shows a hybrid adaptation, where mobility intensity recovers but structural properties remain altered. The Southeast reflects a restructured yet stabilized network with locally cohesive patterns. These results reinforce the importance of disaggregated analysis, showing that regional dynamics do not uniformly mirror national trends and may respond differently to the same policy timeline (Table 1).

Large-scale mobility shifts: Structural changes and network adaptation

The analysis of global components in Mexico's intermunicipal mobility network reveals key insights into large-scale connectivity and the municipalities that function as interregional links. The number of global components fluctuates daily, ranging from 1 to 19, with an average of four per day. The highest number (19) occurs on November 30, 2020, coinciding with the peak number of local components. This pattern suggests a period of heightened fragmentation and localized mobility. Despite these fluctuations, most municipalities consistently belong to a single large global component, even during periods of reduced mobility. The smaller global components that emerge generally consist of isolated connections between pairs of communities. This trend indicates that the primary structure of intermunicipal connectivity in Mexico remains largely encapsulated within the largest global component.

Change point detection analysis identifies key structural shifts over time, marking distinct phases of interregional mobility adaptation (see S4 Fig).

The first major disruption occurs around March 19, 2020, shortly after the first confirmed COVID-19 case in Mexico and the launch of the National Healthy Distance Campaign (March 23). This point coincides with a sharp drop in density and shortest path length, indicating a breakdown in long-range connectivity due to early voluntary reductions in travel, followed by formal restrictions in early April. The transitivity also decreases significantly by late March (detected on Feb 24), suggesting a loss of global cohesion across the network. The second significant transition takes place between late May and early August 2020. During this phase, we observe simultaneous shifts in strength, transitivity, and shortest path, with a detected peak in total strength on August 1. This period follows the initial wave of restrictions and aligns with the beginning of the "New Normality" reopening plan (announced in May and implemented from June 1). However, unlike the local components, which stabilize somewhat during this phase, the global component remains structurally volatile, highlighting an unstable recovery in long-distance mobility. A third restructuring occurs between September and October 2020, with a change in clustering coefficient and average path length (September 21), concurrent with increasing infection rates and the epidemiological alert issued by PAHO/WHO (October 9). This indicates a period of policy re-tightening or voluntary retreat from non-essential travel, consistent with the late-2020 shifts seen in the national and local networks. The final major phase of transformation spans from April to October 2021, marked by successive change points in clustering (April 7), assortativity (April 7 and August 24), and density (May 1). This period corresponds to the progressive vaccination rollout and selective easing of restrictions in Mexico. Although clustering increases, assortativity continues to decline, confirming that while certain regional hubs become locally denser, the global network remains structurally fragmented. This is consistent with what we observe in the national network and local components 3 and 6, where clustering rises but assortativity falls, indicating regionally concentrated but uneven recovery. Interestingly, unlike the national network, which

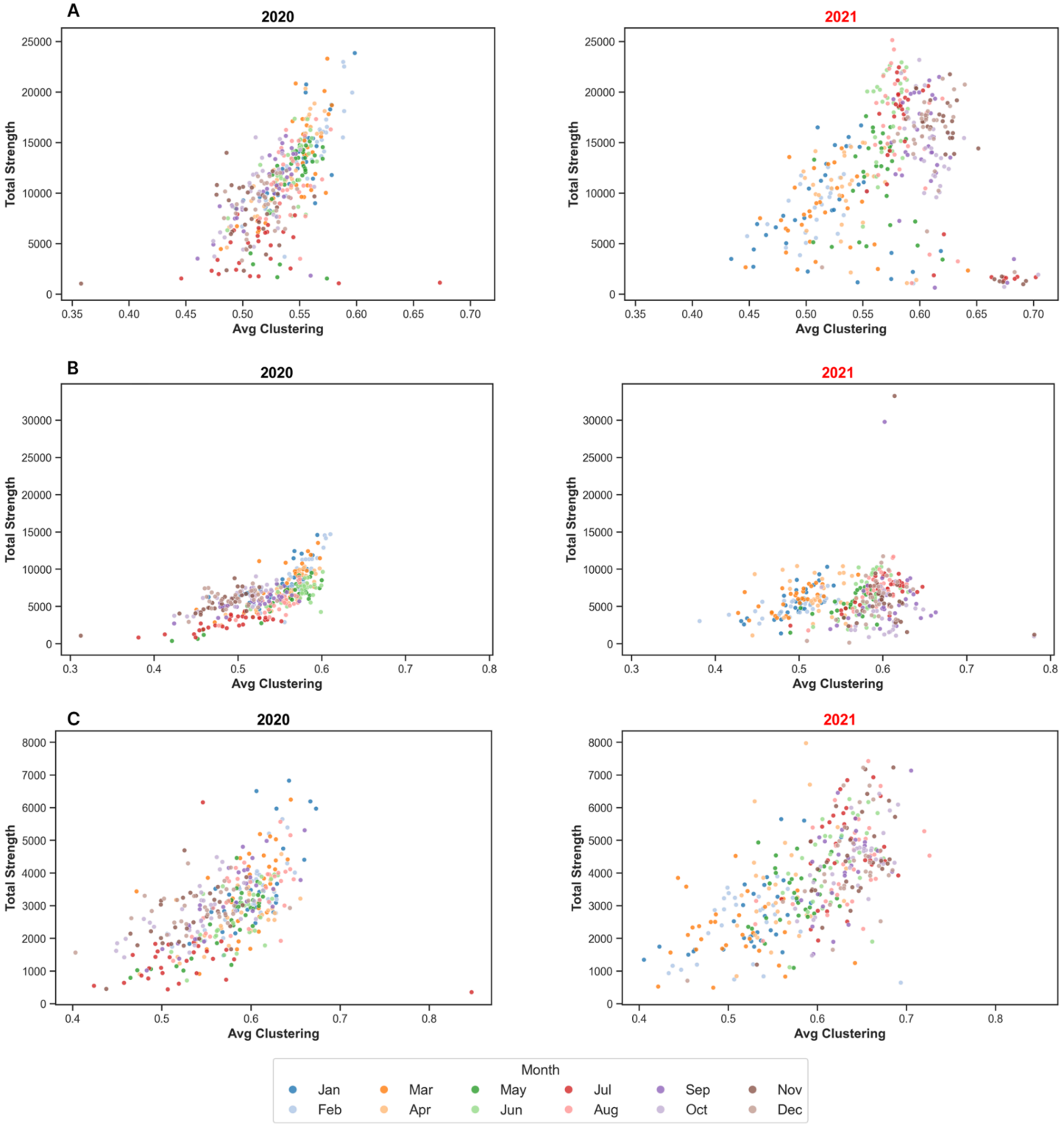

Fig 7. Monthly joint evolution of structural metrics in the local components (2020–2021). Relationship between Total Strength and Average Clustering Coefficient, with data points colored by month. Each subplot shows the relationship between two structural metrics, separately for 2020 (left column) and 2021 (right column). Each dot represents one day, and its color encodes the corresponding month. The monthly color encoding allows us to observe seasonal dynamics, shifts in structural regimes, and changes in variability or dispersion between pandemic phases. (A) represents the West region, (B) represents the South-East region, and (C) represents the North-West region.

https://doi.org/10.1371/journal.pcsy.0000086.g007

shows a last major shift in September 2021 (coinciding with Independence Day), the global component does not reflect a marked re-expansion during that time. Instead, it shows earlier fragmentation (August 24, 2021) and a final structural adjustment in December 2021, well after major public events. In summary, the global component exhibits a series of asynchronous structural transitions. While some change points align with national and regional events, others reflect unique timing, underscoring the differentiated dynamics of long-distance mobility. The persistent decrease in assortativity and fragmented structure suggest that despite recovery in volume, the connectivity patterns of the global mobility layer remain altered beyond the immediate crisis.

Fig 8 illustrates the evolution of long-distance travel between major regional components across key moments of the pandemic. In early 2020 (panel A), before the onset of national restrictions, the intermunicipal mobility network exhibits dense and well-established connections across regions, reflecting typical long-distance travel flows. The snapshot from January 9, 2020, shows robust inter-component interactions, including significant links between central, northern, and southeastern states. By March 23 and April 1, coinciding with the launch of the National Healthy Distance Campaign and the declaration of a national emergency, a notable reduction in long-distance mobility is observed. The visual thinning and removal of many interregional links during this period clearly reflect the impact of policy interventions on travel behavior. Panel B captures the progressive fragmentation of the global component later in 2020. On November 17, subcomponents appear, especially in central and southern Mexico. This date aligns with a period of rising cases and renewed caution following autumn festivities. Two weeks later (November 30), the network appears further fragmented, with diminished long-range connections and a proliferation of smaller regional clusters. These changes reflect the cumulative effects of sustained restrictions and altered travel behavior approaching the holiday season. By December 31, 2020, some long-distance links reemerge, suggesting temporary mobility spikes due to end-of-year travel. This brief resurgence aligns with Christmas holidays and increased familial and social visits, despite ongoing epidemiological risks. In panel C, the network in May 2021 shows a transition toward reorganization and recovery. The period coincides with the expansion of vaccination to broader segments of the population and the progressive easing of restrictions in major cities such as Mexico City (Table 1). Notably, by June 2, the reformation of the global component becomes evident, as previously fragmented regions reconnect through stable long-distance links. These reconnections remain visible in the November 2 map, suggesting a persistent structural reconfiguration—distinct from pre-pandemic patterns. Overall, while the volume of long-distance travel partially rebounds by mid-to-late 2021, the spatial structure of these flows appears altered. The network does not simply revert to its former configuration but instead reorganizes around more cohesive and possibly more resilient interregional pathways. These shifts underscore the long-term impact of the pandemic on spatial mobility systems, where behavioral adaptation, public health interventions, and infrastructure constraints jointly shape the geography of mobility recovery.

Clustering analysis of the global component (Fig 8) reveals three structural mobility regimes. Cluster 1 dominates the early phase of 2020, corresponding to the pre-pandemic structure and initial response. Cluster 2 emerges progressively from April 2020 and dominates until early 2021, capturing the period of maximum disruption. Cluster 3 becomes dominant from mid-2021 onward, reflecting a stabilized recovery phase characterized by renewed cohesion in intermunicipal mobility.

The temporal heatmap (Fig 9B) illustrates these transitions and reveals a clear overlap between clusters, especially between April and August 2020. During this transitional phase, days are distributed across all three clusters. This overlap suggests that structural changes in interregional mobility were neither synchronous nor homogeneous. A similar overlap reoccurs during early 2021, indicating another period of structural uncertainty before recovery becomes the dominant trend.

These overlapping transitions suggest that interregional mobility reorganization followed a gradual, adaptive process rather than abrupt shifts. The delayed dominance of Cluster 3 reinforces the idea that recovery was progressive and uneven across the country. Overall, the coexistence of clusters during key periods highlights the importance of structural

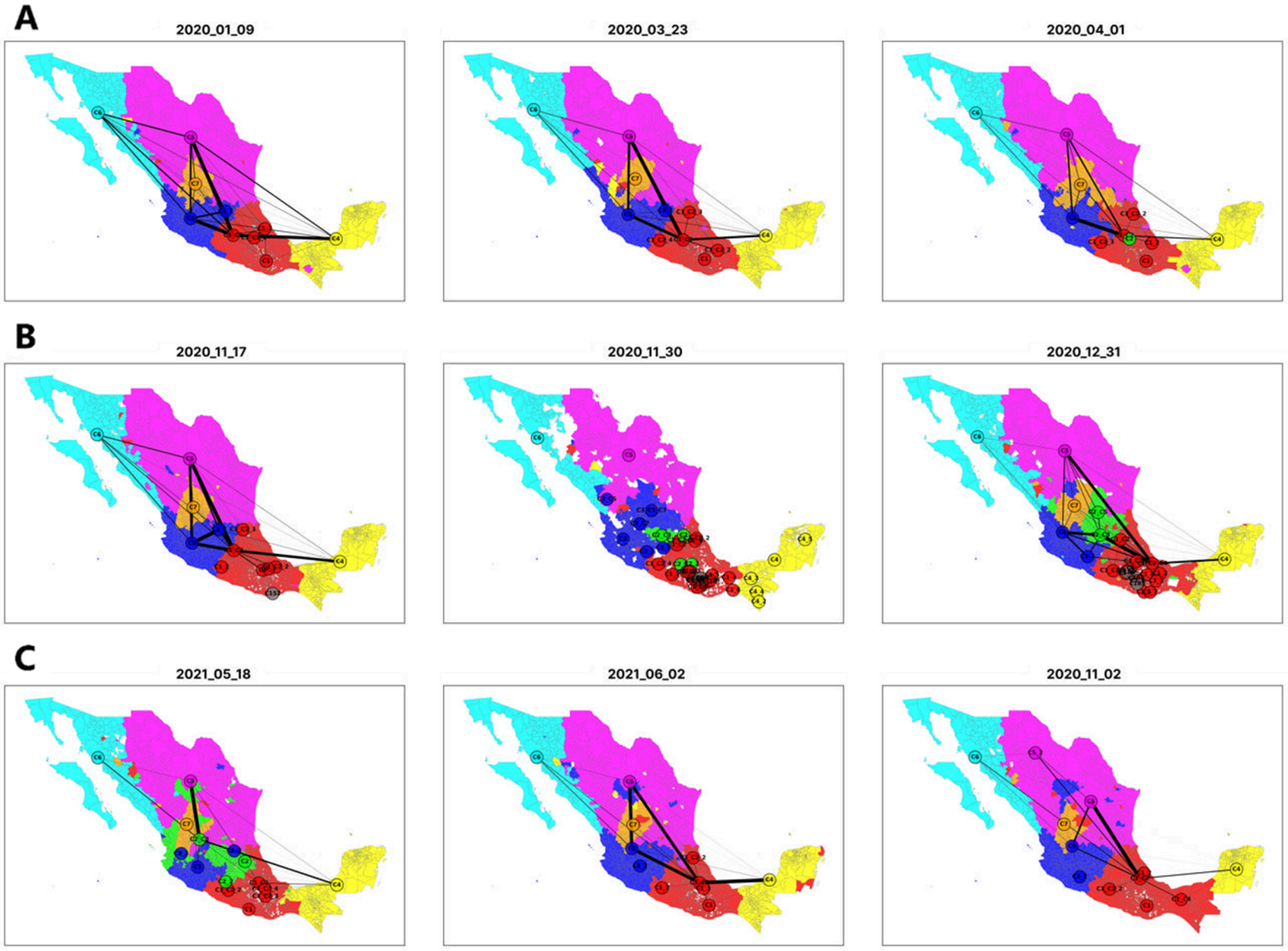

Fig 8. **Selected dates of inter-regional movements.** This visualization highlights the flow of movements between global regions on key dates from 2020 to 2021. Each map displays the geographic distribution of local components detected in the intermunicipal mobility network for a specific date. Colors represent distinct components. The background map provides spatial context, helping to situate municipalities and track their community affiliation over time. (A) Captures the initial response, showing a sharp decline in mobility following government restrictions. (B) Highlights shifts in late 2020, including reduced long-distance travel and increased short-distance movement during the holidays. (C) Reflects mobility stabilization in 2021, with the formation of functional regions in the south, a resurgence of long-distance trips, and increased movement during cultural events like the Day of the Dead. The base map was created with GeoPandas using INEGI's publicly available shapefiles [30].

https://doi.org/10.1371/journal.pcsy.0000086.g008

analysis beyond simple mobility volume and emphasizes the complex interplay between national policies and network reconfiguration.

Overall, what we observe here is that, at the beginning of the pandemic, there was no immediate structural coordination between regions. Long-distance mobility patterns did not reorganize immediately, but reflected the gradual implementation of national public policies. The coexistence of both clusters from April to August 2020 suggests a period of uncertainty, where interregional travel was still adjusting to evolving restrictions. It was only later that a more coherent structural shift occurred.

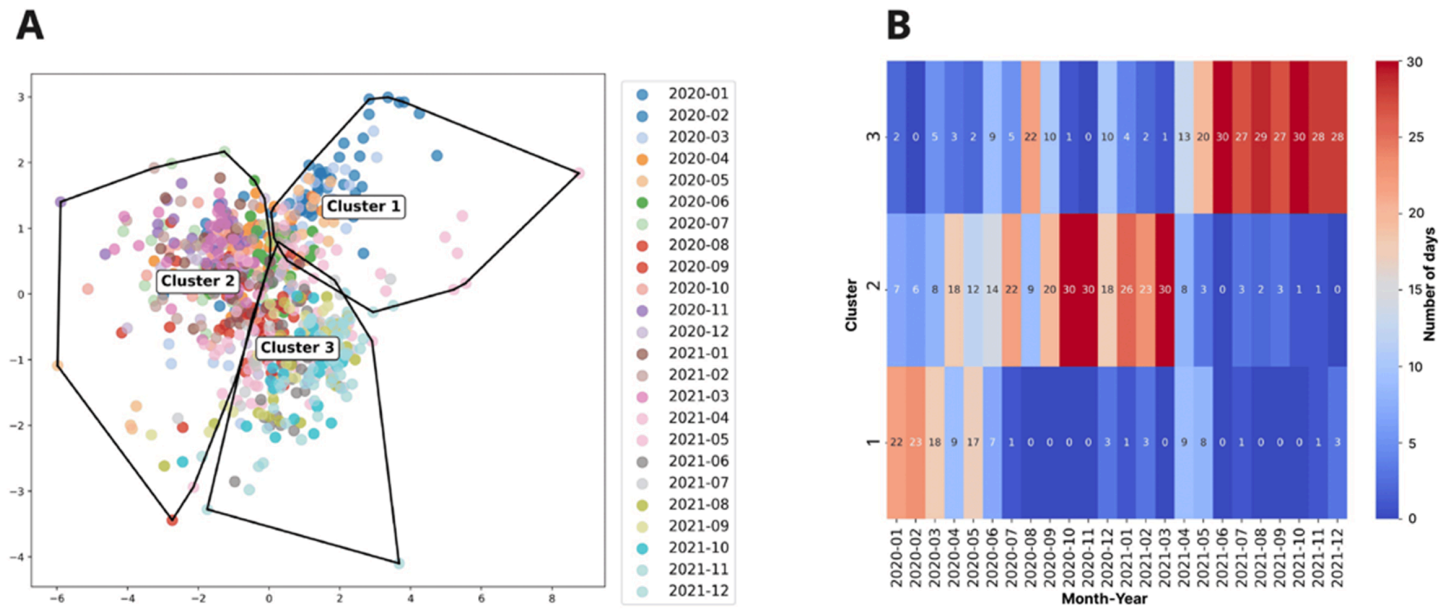

Fig 9. **Temporal evolution of the largest global component of the Mexico intermunicipal mobility network.** (A) Clustering results of daily mobility network structures projected into a reduced-dimensional space. Each point represents a day, colored according to its corresponding month. The black convex hulls indicate the boundaries of the detected clusters. (B) Heatmap showing the temporal distribution of clusters. The x-axis represents months, while the y-axis corresponds to clusters. The color intensity indicates the number of days assigned to each cluster within a given month.

https://doi.org/10.1371/journal.pcsy.0000086.g009

A comparative analysis of network properties further highlights the evolution of large-scale mobility over 2020 and 2021 (Fig 10). In 2020, we observe a strong positive correlation between total strength and density, particularly during the early months (January–March), which precede the onset of national mobility restrictions. The clear color segmentation in the scatter plots (particularly in the first quarter) reflects well-defined monthly patterns in mobility behavior. However, from April onward, following the declaration of the national emergency (April 1) and implementation of strict distancing policies (March 23), both density and strength decline sharply. This results in the formation of a more dispersed distribution of points, indicative of structural fragmentation and reduced long-distance travel. In contrast, during 2021, the temporal clusters observed in 2020 begin to blend. From January to June 2021, coinciding with the rollout of the national vaccination campaign and the gradual lifting of restrictions, the density of interregional connections increases steadily. This reflects a progressive reactivation of travel between regions. Notably, while the overall density approaches pre-pandemic levels, the scatter plot shows greater continuity in point distribution, suggesting that transitions were smoother and more structurally stable.

Looking at the relationship between average clustering coefficient and total strength, the 2020 data show lower and more variable clustering, with values ranging from approximately 0.15 to 0.35. This aligns with the observed disruption of inter-regional travel, where cohesion between distant urban areas weakened. In 2021, clustering values rise more consistently for higher-strength connections, with visible shifts starting around April, shortly after the expansion of vaccine eligibility to teachers and vulnerable populations. This suggests a partial restoration of cohesive mobility structures, particularly along stronger, well-traveled inter-regional routes.

Taken together, these patterns illustrate a trajectory of adaptation: after the initial collapse of large-scale mobility in early 2020, the network gradually reorganized in 2021. While the volume of interregional trips increased and connectivity improved, the structure of travel remained altered. Clustering coefficients were higher, reflecting more tightly knit substructures. Assortativity and heterogeneity in connectivity patterns persisted, pointing to a new configuration of long-distance

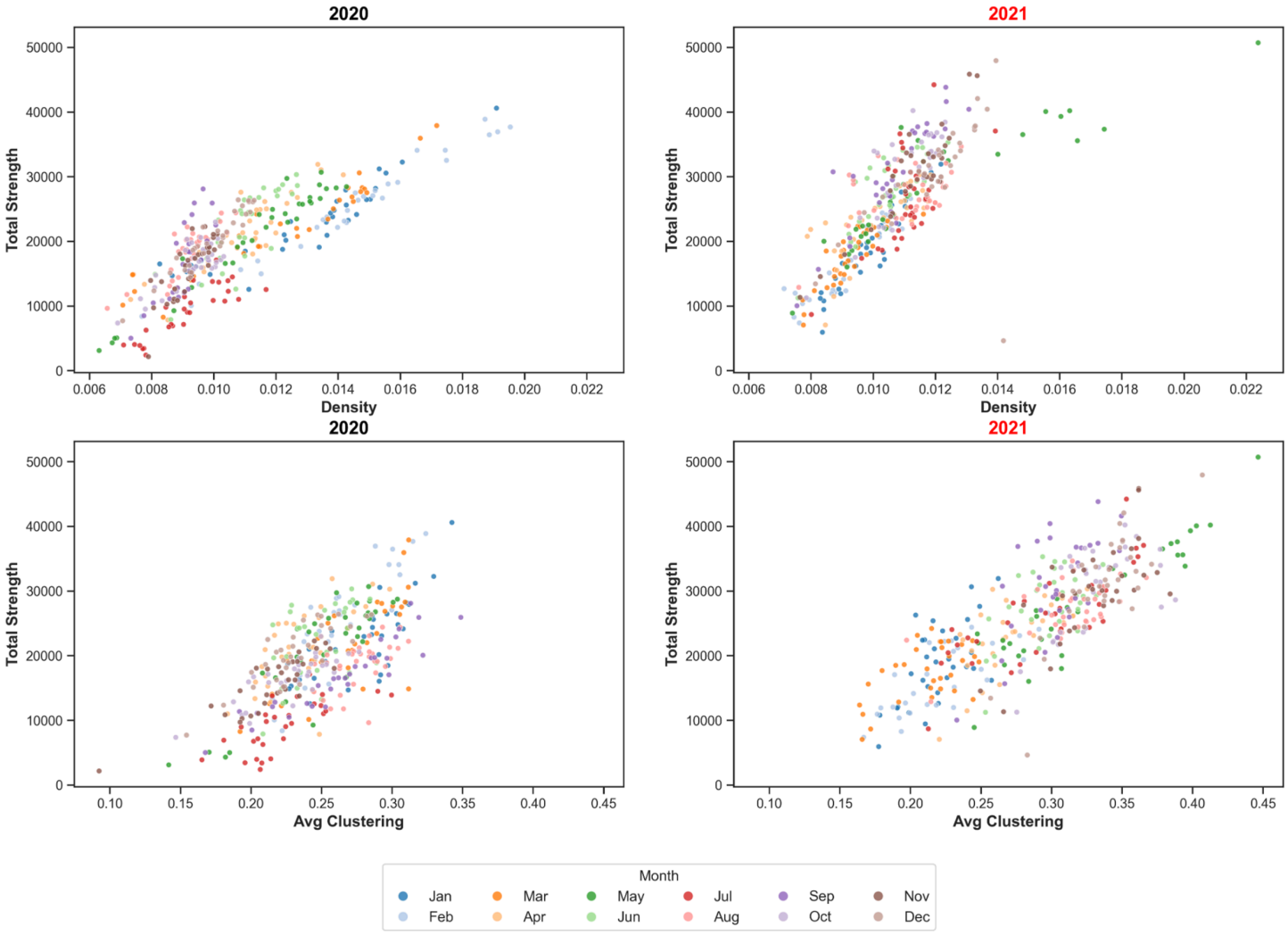

Fig 10. Monthly joint evolution of structural metrics in the large-scale mobility in Mexico (2020–2021). (Top) Scatter plots displaying relationships between Density and Total Strength, showing the evolution of interregional connectivity. (Bottom) Relationship between Total Strength and Average Clustering Coefficient, highlighting changes in network cohesion over time. Each subplot shows the relationship between two structural metrics, separately for 2020 (left column) and 2021 (right column). Each dot represents one day, and its color encodes the corresponding month. The monthly color encoding allows us to observe seasonal dynamics, shifts in structural regimes, and changes in variability or dispersion between pandemic phases.

https://doi.org/10.1371/journal.pcsy.0000086.g010

mobility shaped by behavioral adaptation, risk perception, and public health measures. These findings emphasize that even as mobility resumed, the underlying structure of interregional travel remained transformed, suggesting a long-term shift in how people move across Mexico.

Discussion and perspectives

The COVID-19 pandemic provides an unprecedented natural experiment to study large-scale mobility disruptions and their long-term consequences. This study analyzes Mexico's intermunicipal mobility network across multiple spatial scales to assess how movement patterns change and to what extent they recover. The findings reveal three major phases: pre-pandemic, pandemic, and post-restriction, each characterized by distinct structural shifts in mobility networks. While some

aspects of mobility have returned to near pre-pandemic levels, others exhibit persistent changes. This persistence indicates a lasting impact on travel behavior, urban dynamics, and regional connectivity. Our clustering analyses show that the number of structural regimes varies with scale: we find three regimes when examining the full national network and the largest global component, but only two in several regional components. This means that policy measures and vaccination phases explain part—but not all—of the structural changes, and that each spatial scale responds in its own way to the pandemic's shocks.

One of the clearest takeaways from this study is that mobility is highly adaptive but does not fully revert to previous patterns after a major disruption. Similar to findings in other countries [18,19], mobility in Mexico displays a rapid initial decline in response to lockdowns, followed by a restructuring phase where new connectivity patterns emerged. The persistence of these changes underscores that mobility networks are not only shaped by external shocks like the pandemic but also by long-term shifts in work habits, commuting behavior, and economic activity. The widespread adoption of remote work and digital services reduces daily commuting needs, reshaping urban mobility in lasting ways. Prior studies show that post-restriction work-from-home policies contribute to urban decentralization and increased residential movement toward suburban and peripheral areas [21]. The findings in Mexico align with this trend, particularly in the long-term persistence of altered interregional connections and increased local clustering. This pattern suggests a reinforcement of short-distance travel at the expense of long-distance commuting.

The pandemic reveals that mobility restrictions impact regions unevenly. Some areas recover quickly, while others experience structural mobility changes that persist beyond the pandemic's peak. Regional differences in economic activity, infrastructure, and population density shape the speed and nature of mobility recovery, aligning with findings on urban mobility variations across socioeconomic contexts [22,23]. In Mexico, certain regions maintain a fragmented mobility structure, suggesting that some pre-pandemic intermunicipal connections undergo permanent alterations. These findings indicate that mobility policies should adapt to specific geographic and economic conditions rather than follow a uniform approach. Our regional component analysis reinforces this point: the West shows a near-complete return to its pre-pandemic network structure by mid-2021, the Northwest exhibits a hybrid recovery with persistent topological changes, and the Southeast undergoes a slower, more profound reorganization toward locally cohesive patterns. These contrasting trajectories highlight the need for region-specific policy responses.

Long-term shifts in mobility networks highlight the need for resilient transportation systems that adapt to sudden disruptions. This study emphasizes the importance of flexible public transportation strategies that respond dynamically to demand fluctuations. Research shows that cities with diverse mobility options, such as cycling paths, walkable streets, and decentralized transit, recover faster than those with rigid networks [19]. In Mexico, regional recovery patterns vary significantly, indicating that mobility policies must prioritize adaptability. A flexible approach ensures that transportation systems remain functional during future disruptions. Episodes such as the exceptional fragmentation observed on 30 November 2020—driven by a confluence of a COVID-19 case peak, an airline suspension, and even a solar eclipse—illustrate how cultural events, infrastructure shocks, and epidemiological factors can abruptly alter network structure and should be anticipated in contingency planning.

In addition to transportation policy, the findings also highlight the growing role of digital infrastructure in sustaining economic and social activity during mobility restrictions. The increase in home-based work and online shopping suggests that future urban planning should integrate digital access as a fundamental component of mobility policies. Enhancing digital connectivity in remote and underserved areas could reduce travel demand while maintaining economic productivity. Furthermore, investments in digital infrastructure could help mitigate mobility inequalities by providing alternative means of accessing employment, education, and services without the need for physical movement.

Understanding these long-term mobility shifts also raises important questions for future research. One pressing question is how these changes in movement patterns will affect economic productivity, labor markets, and social interactions in the long run. Mobility networks closely link to economic structures, requiring further study to determine if altered commuting behaviors drive regional economic transformations. Another key avenue for research is the role of behavioral changes

in shaping mobility networks. While infrastructure and policy responses influence recovery, individual choices, such as risk perception, remote work preferences, and travel habits, also play a role. Integrating behavioral models with mobility network analysis could provide a more comprehensive understanding of these dynamics.

Comparative studies across countries and urban systems provide a broader context for Mexico's mobility trends. While some patterns align with findings from other regions, each country's response to the pandemic reflects distinct economic, cultural, and policy factors. A cross-national approach identifies whether mobility adaptations are universal or region-specific. Understanding these variations offers valuable insights for global transportation and urban planning strategies.

Overall, the COVID-19 pandemic reshapes human mobility in Mexico, disrupting movement patterns and causing lasting structural changes in mobility networks. While some aspects recover, persistent shifts in clustering and connectivity indicate that mobility does not fully return to its previous state. These findings highlight the need for resilient and adaptive mobility planning that accounts for long-term disruptions. Lessons from this crisis inform future transportation policies, urban planning strategies, and emergency preparedness, ensuring mobility networks remain robust and adaptable.

Materials and methods

Data

This study utilizes intermunicipal travel networks derived from [23], constructed using anonymized mobile phone location data from Mexico. The network datasets are accessible at https://osf.io/gwq6u/. In these networks, nodes represent municipalities or metropolitan areas in Mexico, identified by their respective codes assigned by the National Institute for Statistics, Geography, and Informatics (INEGI). Edges correspond to the observed mobility of devices traveling from node i to node j. Weights represent the normalized number of devices moving between these locations. The dataset comprises 728 networks, each capturing daily human mobility between municipalities in Mexico from 2020 to 2021. Each network includes 2,446 municipalities and 107 metropolitan zones.

Shapefiles defining the geographical boundaries of municipalities, states, and the country are sourced from INEGI's Geostatistical Framework for the 2020 Population and Housing Census [32]. Additionally, shapefiles delineating metropolitan zones are obtained from [33].

Table 1 provides a detailed timeline of key epidemiological events and public health measures related to the COVID-19 pandemic in Mexico from December 2019 to January 2021 [27,34,35]. This chronology serves as essential contextual information to interpret structural shifts observed in the mobility network. Notably, the timeline highlights the initial spread of the virus, the declaration of national emergency phases, and the implementation of major containment strategies such as the "National Healthy Distance Campaign." It also includes symbolic or behaviorally impactful events (e.g., Day of the Dead, Christmas celebrations), and the launch of Mexico's vaccination campaign.

Clustering approach

To identify patterns in the temporal evolution of Mexico's intermunicipal mobility network, we perform clustering on topological feature vectors computed for each daily network. As illustrated in Fig 11, we begin by extracting a set of structural metrics from each temporal snapshot of the network. These initial features include seven core topological properties: Density, Total Strength, Average Clustering Coefficient, Assortativity, Transitivity, Diameter, Average Shortest Path Length.

To avoid redundancy and mitigate multicollinearity, we compute the Pearson correlation coefficients among all selected features. We then discard features exhibiting strong linear correlation, defined as $|r| > 0.75$, keeping only those that contribute distinct structural information. This filtering step ensures that the clustering captures diverse and non-overlapping aspects of the network's topology. The corresponding correlation matrices for different network scales (global, local components, full network) are provided in the Supporting Information (S5 Fig and S6 Fig).

Each daily network is thus represented as a feature vector in a reduced, decorrelated metric space. Aggregating these vectors over time yields a feature matrix, where rows correspond to days and columns to retained topological

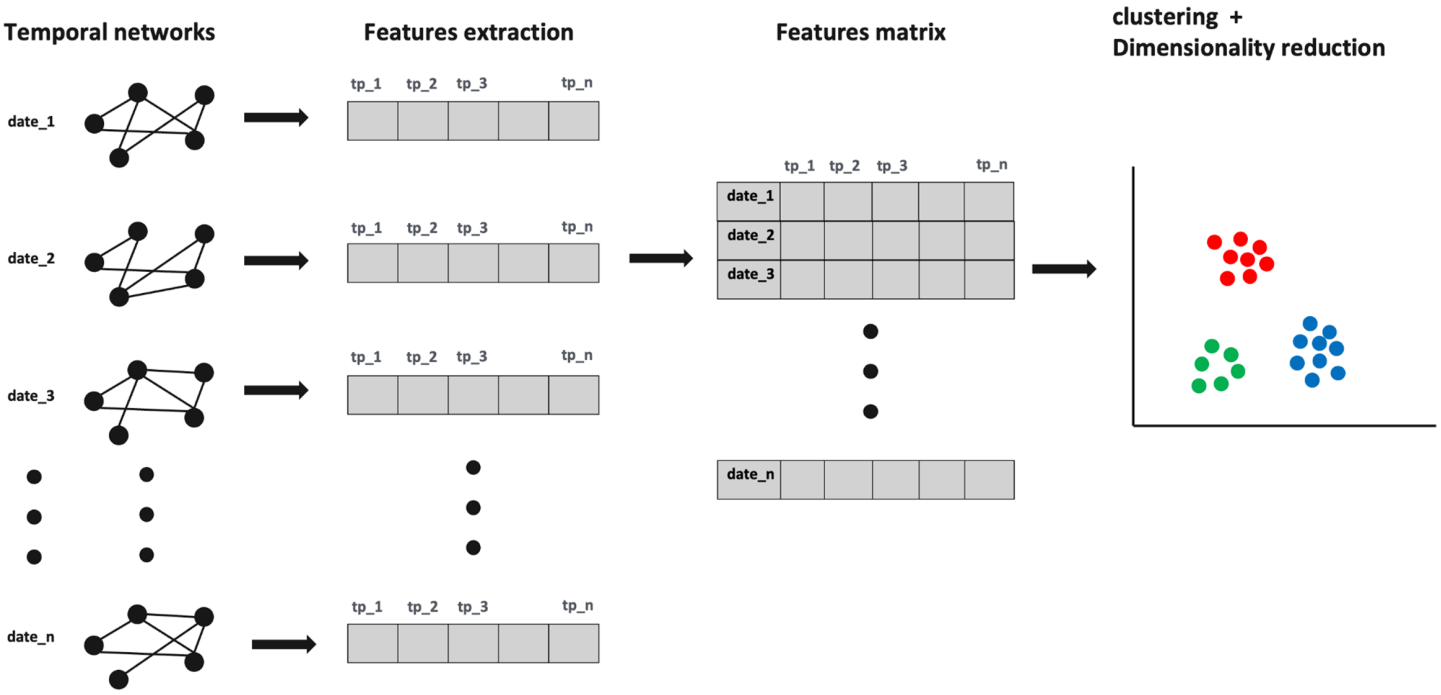

Fig 11. Clustering pipeline: from daily temporal networks to structural feature extraction, feature matrix construction, and clustering with dimensionality reduction. Each day is represented as a point in topological space and assigned to a structural regime.

https://doi.org/10.1371/journal.pcsy.0000086.g011

properties. This matrix serves as input for a k-means clustering algorithm, aimed at grouping days with similar structural configurations.

The optimal number of clusters was determined using a silhouette score analysis, which evaluates the performance of the cluster based on the similarity between groups. Among the values tested ($k = 2$ to $k = 6$). One can see the silhouette score in the Supporting Information (S7 Fig and S8 Fig). To facilitate visualization, we project the high-dimensional feature space into two dimensions using Principal Component Analysis (PCA). This reveals compact and well-separated clusters, indicating distinct network regimes.

To examine how these structural patterns evolve over time, we generate a monthly heatmap that shows the distribution of cluster memberships across the entire observation period. This temporal mapping allows us to track shifts in mobility structure and to associate network regimes with policy interventions and pandemic phases.

Change point detection

To detect structural changes in the mobility network over time, we apply change point detection to daily univariate time series derived from individual topological metrics. Each metric (e.g., density, average strength, clustering coefficient, assortativity) is analyzed separately. These metrics are computed from weighted and directed intermunicipal mobility networks, where edge weights $w_{ij}(t)$ represent the normalized number of observed trips from municipality i to j on day t, based on anonymized mobile phone data.

We adopt the non-parametric `KernelCPD` algorithm from the `ruptures` library [36], which does not assume any specific statistical distribution within segments. Unlike parametric models such as `"l2"`, which rely on a constant mean assumption, kernel-based methods are well-suited to detecting complex and non-linear shifts in univariate time series.

We use a **linear kernel**, defined as:

$$K(x_i, x_j) = \exp\left(-\lambda |x_i - x_j\|^2\right),$$

where $\langle \cdot, \cdot \rangle$ denotes the standard dot product. This kernel provides a simple and efficient measure of similarity between observations. Given a segment $s = \{x_i, \ldots, x_j\}$, the segment cost is computed as:

$$c(s) = \frac{1}{(j-i)^2} \sum_{p=i}^{j} \sum_{q=i}^{j} K(x_p, x_q),$$

which quantifies the internal cohesion of the segment. The total segmentation cost is minimized by selecting breakpoints that best preserve similarity within segments.

Since `KernelCPD` requires the number of breakpoints to be specified in advance, we set $n_{\text{bkps}} = 3$. This choice is supported by several considerations. First, visual inspection of structural metric trajectories suggests three dominant transitions throughout the 2020–2021 period. Increasing this number led to closely spaced or redundant breakpoints, indicative of over-segmentation and reduced interpretability. Second, the three-phase structure aligns with major contextual events: the pre-pandemic baseline, the period of strict mobility restrictions, and the post-restriction adjustment phase. Third, applying change point detection across different structural metrics yields consistent breakpoint locations, reinforcing the robustness of the selected value. Together, these factors validate the use of $n_{\text{bkps}} = 3$ as a parsimonious yet meaningful segmentation of the mobility network's temporal evolution.

Component structure extraction

The extraction of global and local components follows the methodology described in [24,37]. This approach is based on the premise that networks contain dense, localized regions where nodes primarily interact within their community. The network is divided into two sets: local components, which are dense regions that share information internally, and global components, which consist of nodes and links connecting different local components. The extraction algorithm consists of three main steps:

1. Identify Dense Regions: Apply a community detection algorithm to reveal the network's community structure.
2. Extract Local Components: Isolate local components by removing inter-community links from the identified community structure.
3. Extract Global Components: Remove intra-community links and any isolated nodes to extract the global components.

In this work we uses the Louvain community detection algorithm [38] applied to a daily network for the two years.

Topological metrics

We compute several network-level metrics to characterize the structural properties of the daily intermunicipal mobility networks. All metrics are calculated on **weighted and directed graphs**, where the edge weight $w_{ij}(t)$ denotes the normalized number of observed trips from municipality i to j on day t. The definitions are as follows:

- **Network Density.** The density quantifies the fraction of actual connections out of all possible directed connections:

$$D(t) = \frac{E(t)}{N(t)(N(t)-1)},$$

where $E(t)$ is the number of observed edges and $N(t)$ is the number of active nodes on day t. It provides a measure of the network's global connectivity.

- **Node Strength.** The strength of a node is defined as the sum of weights on its incident edges. We consider:
  - In-strength: sum of incoming edge weights.
  - Out-strength: sum of outgoing edge weights.
  - Total strength of the network:

$$S(t) = \sum_{i,j} w_{ij}(t),$$

  which reflects the overall mobility intensity on day t.
- **Average Shortest Path Length.** This metric represents the average number of steps along the shortest paths between all pairs of reachable nodes. In the weighted case, edge weights are treated as inverse distances:

$$d_{ij} = \frac{1}{w_{ij}(t)}.$$

  The average is computed over all pairs in the largest strongly connected component.
- **Diameter.** The diameter is the maximum shortest path length among all node pairs in the largest connected component:

$$\text{Diameter}(t) = \max_{i,j} d_{ij}(t).$$

- **Average Clustering Coefficient.** The clustering coefficient of a node quantifies the tendency of its neighbors to be connected. In the weighted, directed case, we adapt the classical formulation to include edge directions and weights. The average clustering coefficient is then:

$$C(t) = \frac{1}{N'} \sum_{i \in V'} c_i(t),$$

  where $V' \subseteq V$ includes all nodes with degree at least 2, and $c_i(t)$ is the local clustering coefficient of node i at time t.
- **Transitivity.** This global clustering measure is defined as the ratio of closed triplets to all triplets in the network:

$$T(t) = \frac{3 \times \text{Number of Triangles}}{\text{Number of Connected Triplets}}.$$

- **Assortativity.** Assortativity reflects the correlation between node degrees (or strengths) at either end of an edge. It is computed for weighted, directed networks using the Pearson correlation coefficient between the strengths of connected node pairs.

Supporting information

S1 Fig. Comparative analysis of the stable local components. Relationship between Total Strength and density, with data points colored by month. (A) represents the West region, (B) represents the South-East region, and (C) represents the North-West region.
(TIFF)

S2 Fig. Temporal evolution of the local component in the South-East region with detected change points. Each subplot represents a different metric, with the x-axis indicating time (dates) and the y-axis showing respective metric values. Red dashed vertical lines highlight significant change points annotated with their corresponding dates.
(TIFF)

S3 Fig. Temporal evolution of the local component in the North-West region with detected change points. Each subplot represents a different metric, with the x-axis indicating time (dates) and the y-axis showing respective metric values. Red dashed vertical lines highlight significant change points annotated with their corresponding dates.
(TIFF)

S4 Fig. Temporal evolution of the largest global component with detected change points. Each subplot represents a different metric, with the x-axis indicating time (dates) and the y-axis showing respective metric values. Red dashed vertical lines highlight significant change points annotated with their corresponding dates.
(TIFF)

S5 Fig. Correlation matrices of the Mexico mobility network and the global component. Pearson correlation matrices between topological features for three local components of the intermunicipal mobility network. The number of retained features after redundancy filtering ($|r| > 0.75$) varies between networks. (A) represents the Mexico mobility network, and (B) represents the global component.
(TIFF)

S6 Fig. Correlation matrices of local components. Pearson correlation matrices between topological features for three local components of the intermunicipal mobility network. The number of retained features after redundancy filtering ($|r| > 0.75$) varies between components. (A) represents the West region, (B) represents the South-East region, and (C) represents the North-West region.
(TIFF)

S7 Fig. Silhouette scores for different values of *k* in clustering for the Mexico mobility network and the global component. Silhouette scores are computed for $k = 2$ to $k = 5$ to evaluate clustering performance. The maximum score is obtained for $k = 2$ and $k = 3$, justifying the selection of three distinct structural regimes in the temporal evolution. (A) represents the Mexico intermunicipal mobility network, and (B) represents the global component.
(TIFF)

S8 Fig. Silhouette scores for different values of *k* in clustering of the three stable mobility components. Silhouette scores are computed for $k = 2$ to $k = 5$ to evaluate clustering performance. The maximum score is obtained for $k = 2$, justifying the selection of two distinct clusters in the temporal evolution of the stable local components.
(TIFF)

Acknowledgments

This project was supported by the Fondo Conjunto de Cooperación México-Uruguay from the Agencia Uruguaya de Cooperación Internacional and the Agencia Mexicana de Cooperación Internacional para el Desarrollo.

Author contributions

Conceptualization: Issa Moussa Diop, Hocine Cherifi, Maribel Hernandez-Rosales.

Data curation: Issa Moussa Diop, Erika Cruz-Bonilla.

Formal analysis: Issa Moussa Diop, Erika Cruz-Bonilla, Maribel Hernandez-Rosales.

Funding acquisition: Maribel Hernandez-Rosales.

Investigation: Hocine Cherifi, Maribel Hernandez-Rosales.

Methodology: Issa Moussa Diop, Erika Cruz-Bonilla, Christian Wolff, Maribel Hernandez-Rosales.

Project administration: Maribel Hernandez-Rosales.

Supervision: Maribel Hernandez-Rosales.

Visualization: Issa Moussa Diop, Erika Cruz-Bonilla.

Writing – original draft: Issa Moussa Diop, Erika Cruz-Bonilla, Maribel Hernandez-Rosales.

Writing – review & editing: Christian Wolff, Hocine Cherifi, Maribel Hernandez-Rosales.

References

1. Barbosa H, Barthelemy M, Ghoshal G, James CR, Lenormand M, Louail T, et al. Human mobility: models and applications. Physics Reports. 2018;734:1–74. https://doi.org/10.1016/j.physrep.2018.01.001
2. Pappalardo L, Manley E, Sekara V, Alessandretti L. Future directions in human mobility science. Nat Comput Sci. 2023;3(7):588–600. https://doi.org/10.1038/s43588-023-00469-4 PMID: 38177737
3. Flores-Garrido M, de Anda-Jáuregui G, Guzmán P, Meneses-Viveros A, Hernández-Álvarez A, Cruz-Bonilla E, et al. Mobility networks in Greater Mexico City. Sci Data. 2024;11(1):84. https://doi.org/10.1038/s41597-023-02880-y PMID: 38238306
4. Fang Z, Yang Y, Yang G, Xian Y, Zhang F, Zhang D. CellSense: Human mobility recovery via cellular network data enhancement. Proceedings of the ACM on Interactive, Mobile, Wearable and Ubiquitous Technologies. 2021;5(3):1–22.
5. Zhou X, You L, Zhong S, Cai M. From cell tower location to user location: understanding the spatial uncertainty of mobile phone network data in human mobility research. Computers, Environment and Urban Systems. 2024;111:102130. https://doi.org/10.1016/j.compenvurbsys.2024.102130
6. Chang S, Pierson E, Koh PW, Gerardin J, Redbird B, Grusky D, et al. Mobility network models of COVID-19 explain inequities and inform reopening. Nature. 2021;589(7840):82–7. https://doi.org/10.1038/s41586-020-2923-3 PMID: 33171481
7. Cheng Y, He S, Shao C, Li C, Chen J. Sustainable covid-19 policy responses with urban mobility network epidemic models. IEEE Transactions on Computational Social Systems. 2024.
8. Alessandretti L. What human mobility data tell us about COVID-19 spread. Nat Rev Phys. 2022;4(1):12–3. https://doi.org/10.1038/s42254-021-00407-1 PMID: 34877474
9. Edsberg Møllgaard P, Lehmann S, Alessandretti L. Understanding components of mobility during the COVID-19 pandemic. Philos Trans A Math Phys Eng Sci. 2022;380(2214):20210118. https://doi.org/10.1098/rsta.2021.0118 PMID: 34802271
10. Buchel O, Ninkov A, Cathel D, Bar-Yam Y, Hedayatifar L. Strategizing COVID-19 lockdowns using mobility patterns. R Soc Open Sci. 2021;8(12):210865. https://doi.org/10.1098/rsos.210865 PMID: 34966552
11. Schindler DJ, Clarke J, Barahona M. Multiscale mobility patterns and the restriction of human movement. R Soc Open Sci. 2023;10(10):230405. https://doi.org/10.1098/rsos.230405 PMID: 37830024
12. Shi L, Chi G, Liu X, Liu Y. Human mobility patterns in different communities: a mobile phone data-based social network approach. Annals of GIS. 2015;21(1):15–26. https://doi.org/10.1080/19475683.2014.992372
13. Hossmann T, Spyropoulos T, Legendre F. A complex network analysis of human mobility; 2011. p. 876–81.
14. Bello-Chavolla OY, Antonio-Villa NE, Valdés-Ferrer SI, Fermín-Martínez CA, Fernández-Chirino L, Vargas-Vázquez A, et al. Effectiveness of a nationwide COVID-19 vaccination program in Mexico against symptomatic COVID-19, hospitalizations, and death: a retrospective analysis of national surveillance data. Int J Infect Dis. 2023;129:188–96. https://doi.org/10.1016/j.ijid.2023.01.040 PMID: 36775188
15. Pan Y, Darzi A, Kabiri A, Zhao G, Luo W, Xiong C, et al. Quantifying human mobility behaviour changes during the COVID-19 outbreak in the United States. Sci Rep. 2020;10(1):20742. https://doi.org/10.1038/s41598-020-77751-2 PMID: 33244071
16. Yabe T, Tsubouchi K, Fujiwara N, Wada T, Sekimoto Y, Ukkusuri SV. Non-compulsory measures sufficiently reduced human mobility in Tokyo during the COVID-19 epidemic. Sci Rep. 2020;10(1):18053. https://doi.org/10.1038/s41598-020-75033-5 PMID: 33093497
17. Lee K-S, Eom JK. Systematic literature review on impacts of COVID-19 pandemic and corresponding measures on mobility. Transportation (Amst). 2023:1–55. https://doi.org/10.1007/s11116-023-10392-2 PMID: 37363373
18. Bouzaghrane MA, Obeid H, González M, Walker J. Human mobility reshaped? Deciphering the impacts of the Covid-19 pandemic on activity patterns, spatial habits, and schedule habits. EPJ Data Sci. 2024;13(1):1–20. https://doi.org/10.1140/epjds/s13688-024-00463-4
19. Albalate D, Bel G, Gragera A. Mobility, environment and inequalities in the post-COVID city. Cambridge Journal of Regions, Economy and Society. 2022;15(3):459–75. https://doi.org/10.1093/cjres/rsac021

20. Zhao B, Wang X, Zhang T, Shi R, Xu F, Man F, et al. Estimating and modeling spontaneous mobility changes during the COVID-19 pandemic without stay-at-home orders. Humanit Soc Sci Commun. 2024;11(1). https://doi.org/10.1057/s41599-024-03068-4
21. Li H, Wei YD. COVID-19, cities and inequality. Appl Geogr. 2023;160:103059. https://doi.org/10.1016/j.apgeog.2023.103059 PMID: 37841058
22. Santana C, Botta F, Barbosa H, Privitera F, Menezes R, Di Clemente R. COVID-19 is linked to changes in the time-space dimension of human mobility. Nat Hum Behav. 2023;7(10):1729–39. https://doi.org/10.1038/s41562-023-01660-3 PMID: 37500782
23. Fontanelli O, Guzmán P, Meneses-Viveros A, Hernández-Alvarez A, Flores-Garrido M, Olmedo-Alvarez G, et al. Intermunicipal travel networks of Mexico during the COVID-19 pandemic. Sci Rep. 2023;13(1):8566. https://doi.org/10.1038/s41598-023-35542-5 PMID: 37237051
24. Diop IM, Cherifi C, Diallo C, Cherifi H. Revealing the component structure of the world air transportation network. Appl Netw Sci. 2021;6(1):92. https://doi.org/10.1007/s41109-021-00430-2 PMID: 34841043
25. Dirección de Información Epidemiológica GdM Secretaría de Salud. 31° Informe Epidemiológico de la Situación de COVID-19; 2021. https://www.gob.mx/cms/uploads/attachment/file/668356/Informe_COVID-19_2021.09.13.pdf
26. Secretaría de Salud GdM. Línea del tiempo COVID-19. 2021. https://www.ssm.gob.mx/portal/descargables/vigilancia/2021/Temas_Interes_Epidemiologico/12.-LineaDelTiempoCOVID-19_16MAR2021.pdf
27. COVID-19 CU. Línea del tiempo COVID-19 en México. 2021. https://www.comisioncovid.mx/linea-del-tiempo.html
28. Wikipedia Contributors. Anexo: cronología de la pandemia de COVID-19 en México. https://es.wikipedia.org/wiki/Anexo:Cronolog
29. Jornada L. La jornada. 2020. https://www.jornada.com.mx/2020/11/30/
30. Instituto Nacional de Estadística y Geografía INEGI. Marco Geoestadístico. Censo de Población y Vivienda 2020. https://www.inegi.org.mx/app/biblioteca/ficha.html?upc=889463807469
31. Wikipedia Contributors. Regiones de México. [cited 21 Oct 2023]. https://es.wikipedia.org/wiki/Regiones_de_México
32. INEGI IN de E Geografía e Informática. Marco geoestadístico. Censo de población y vivienda 2020. Aguascalientes, México: INEGI; 2020.
33. de Desarrollo Social S, de Estadística y Geografía IN, de Poblacion CN. Delimitación de las zonas metropolitanas de México. 2010. http://www.conapo.gob.mx/es/CONAPO/Datos_Abiertos_Delimitacion_de_Zonas_Metropolitanas
34. de la Ciudad de México G. Reportes de movilidad y medidas durante festividades 2021; 2021. https://www.covid19.cdmx.gob.mx/
35. de la Federación DO. Semáforo epidemiológico COVID-19. Gobierno de México; 2021. https://www.dof.gob.mx/
36. Truong C, Oudre L, Vayatis N. Selective review of offline change point detection methods. Signal Processing. 2020;167:107299. https://doi.org/10.1016/j.sigpro.2019.107299
37. Cherifi H, Palla G, Szymanski BK, Lu X. On community structure in complex networks: challenges and opportunities. Appl Netw Sci. 2019;4(1):117. https://doi.org/10.1007/s41109-019-0238-9
38. Blondel VD, Guillaume J-L, Lambiotte R, Lefebvre E. Fast unfolding of communities in large networks. J Stat Mech. 2008;2008(10):P10008. https://doi.org/10.1088/1742-5468/2008/10/p10008